

# Integrated Network Pharmacology and Metabolomics Analysis to Reveal the Potential Mechanism of Siwu Paste on Aplastic Anemia Induced by Chemotherapy Drugs

Dan He<sup>1</sup>, Wan Dan<sup>1</sup>, Qing Du<sup>1</sup>, Bing-Bing Shen<sup>1</sup>, Lin Chen<sup>1</sup>, Liang-zi Fang<sup>1</sup>, Jian-Jun Kuang<sup>1</sup>, Chun-yu Tang<sup>2</sup>, Ping Cai<sup>1</sup>, Rong Yu<sup>1,3</sup>, Shui-han Zhang<sup>1</sup>, Jian-hua Huang<sup>1,3</sup>

<sup>1</sup>Hunan Academy of Chinese Medicine, Hunan University of Chinese Medicine, Changsha, Hunan, 410013, People's Republic of China; <sup>2</sup>Hunan Times Sunshine Pharmaceutical Co., Ltd., Changsha, Hunan, 425007, People's Republic of China; <sup>3</sup>Hunan Key Laboratory of TCM Prescription and Syndromes Translational Medicine Hunan, Changsha, Hunan, 410208, People's Republic of China

Correspondence: Shui-han Zhang; Jian-hua Huang, Hunan Academy of Chinese Medicine, Hunan University of Chinese Medicine, Changsha, Hunan, 410013, People's Republic of China, Tel +86 13637400650; +86 18692265317, Email zhangshuihan0220@126.com; huangjianhua1985@163.com

**Purpose:** This study aimed to reveal the multicomponent synergy mechanisms of SWP based on network pharmacology and metabolomics for exploring the relationships of active ingredients, biological targets, and crucial metabolic pathways.

**Materials:** Network pharmacology, including TRRUST, GO, and KEGG, enrichment was used to discover the active ingredients and potential regulation mechanisms of SWP. LC-MS and multivariate data analysis method were further applied to analyze serum metabolomics profiling for discovering the potential metabolic mechanisms of SWP on AA induced by Cyclophosphamide (CTX) and 1-Acetyl-2-phenylhydrazine (APH).

**Results:** A total of 27 important bioactive ingredients meeting the ADME (absorption, distribution, metabolism, and excretion) screening criteria from SWP were selected. Interaction networks were constructed and validated based on the 10 associated ingredients with the relevant targets. A total of 125 biomarkers were found by Metabolomics approach, which associated with the development of AA, mainly involved in amino acid metabolism and lipid metabolism. While SWP can reverse the above 12 metabolites changed by AA. Network analysis revealed the synergistic effects of SWP through the 43 crucial pathways, including Sphingolipid signaling pathway, Sphingolipid metabolism, Arginine and proline metabolism, VEGF signaling pathway, Estrogen signaling pathway.

**Conclusion:** The study suggested that SWP is a useful alternative for the treatment of AA induced by CTX + APH. Its potential mechanisms are to improve hematopoietic microenvironment and promote bone marrow hematopoiesis therapies.

**Keywords:** aplastic anemia, Siwu Paste, network pharmacology, metabolomics, integration analysis

## Introduction

Aplastic anemia (AA), a bone marrow hematopoietic failure (BMF) syndrome, is characterized by attenuated bone marrow hematopoietic cell proliferation, decreased peripheral whole blood cell and immune dysfunction.<sup>1</sup> It has high prevalence in the Asian population, especially young adults.<sup>2</sup> Chemotherapy is the most common cause of AA. Although the immunosuppressive therapy provide an strategy for patients who are not suitable for allogeneic hematopoietic stem cell transplant, some patients after treated with a single therapeutic method show relapse or poor efficacy.<sup>3,4</sup> Therefore, expanding an alternative and more effective therapy for AA is needed. Moreover, the pathogenesis of AA induced by chemotherapy drugs is complex, and combination therapy may supply better service for it than monotherapy.

Siwu Paste (SWP), a popular prescription for tonifying blood, has over 1000 years history in the clinical application of Traditional Chinese Medicine (TCM). It described as good effects in promoting blood circulation, ameliorating anemia and pain, with the feature of, including four herbs: *Angelica sinensis* (Oliv.) Diels (Dang Gui, DG), *Ligusticum chuanxiong* Hort.

(Chuan Xiong, CX), *Cynanchum otophyllum* Schneid.(Bai Shao, BS) and *Rehmanniae radix* preparata (Shu Di Huang, SDH), in the ratio of 10:6:10:15, respectively.<sup>5</sup> Our previous research suggested that SWP may alleviates hematopoietic functions via “multi-component and multichannel”, such as regulating the bone marrow hematopoiesis, improving blood rheology, inhibiting inflammation and exerting estrogen-like effects.<sup>6,7</sup> Compared with other manners, paste is more convenient to carry. And it has better treatment compliance and lower economic burden in treatment of AA induced by chemotherapy drugs. Moreover, SWP at dose of 22.68g/kg has similar efficacy as Fu-Fang E’jiao Jiang.<sup>6</sup> Although, the efficacy of SWP has been demonstrated, the potential mechanism of therapeutic effects of SWP on AA remains puzzled. It limits the application of SWP in experiment as well as clinic. Thus, a comprehensive study is necessary for discovering the relationships among the active ingredient, potential targets, and their molecular mechanisms of SWP in treating AA.

As a promising approach to discover TCM, network pharmacology links the chemical space of drugs to the biomolecular pathways of disease through network footprints. Li et al, conducted a network pharmacology analysis of Danggui Buxue Decoction and they found that the four chemical components (Z-ligustilide, E-butylidenephthalide, Z-butylidenephthalide and ferulic acid) played a major role in the blood enrichment effect.<sup>8</sup> Wang et al, have demonstrated that tetramethylpyrazine and paeoniflorin enable the vessel to sprout by up-regulating ESR $\alpha$  mRNA expression.<sup>9</sup> These studies provide a better basis for our understanding of AA, but network analysis alone cannot truly reflect the impact of multi-component SWP on the occurrence and development of AA. As a systematic method, metabolomics provides a series of particular and sensitive markers for disease diagnosis and drug treatment. The differences between AA patients and healthy, and the therapeutic effects of TCM on AA were studied. Zhong et al, analyzed the difference of serum metabolites between 40 healthy control and 40 AA patients. Comparing with the control groups, they found that the levels of aminoacyl-tRNA biosynthesis, ATP binding cassette transporters, and amino acid biosynthesis were increased markedly in AA, while the TCA cycles was decreased dramatically.<sup>10</sup> Liet al, employed GC/MS technology to provide an evidence that *Angelica sinensis* intervene 5 metabolic pathways (Arachidonic acid metabolism, citrate cycle (TCA), glycine, serine and threonine metabolism, arginine and L-proline metabolism and valine, leucine and isoleucine biosynthesis) to repair the metabolic disorders resulted from AA.<sup>11</sup> He et al, speculate that SWP down-regulate the levels of 3 amino acids (L-Methionine, L-Tyrosine, and L-Phenylalanine) in plasma metabolites compared with AA model group, but it up-regulate the Hippuric acid, Deoxycholic acid and Sphingosine-1-phosphate which are potential therapeutic pathway for AA.<sup>12</sup> Thus, integrated network pharmacology and metabolomics Analysis may provide us an in-depth understanding for SWP in treating AA.

Our study was the first to identify the combinational rules of SWP from molecular and systematic level by integrated network pharmacology and metabolomics analysis, along with pharmacology experiments, to elucidate its therapeutic mechanism for AA induced by chemotherapy drugs.

## Materials and Methods

### Equipment, Chemicals and Reagents

The SWP products were generously provided by Hunan Jiudian Pharmaceutical Co., Ltd. (Hunan, China). In order to obtain reliable experiment results, the preparation and quality control (QC) of SWP were monitored according to our previous research.<sup>6</sup> 2-Chloro-L-phenylalanine, as internal standards for metabolomics analysis, was purchased from Shanghai HC Biotech Co., Ltd. (Shanghai, China) and Avanti (USA) respectively. Q-Exactive LC-MS/MS (Thermo Fisher Scientific) Acetonitrile, methanol, formic acid and LC-MS grade water were purchased from CNW Technologies GmbH (Düsseldorf, Germany).

### Animal

Our tests adhere to the Chinese national laws and local guidelines. Animal experiment has been authorized by the Animal Ethics Committee at Hunan Academy of Chinese Medicine (No.20190030). Healthy Male Sprague Dawley (SD) rat (8 weeks old, weighing 180–220 g) were purchased from Hunan SJA Laboratory Animal Co., Ltd (SCXK 2016–0002). Before the experiment, 30 rats were randomly divided into 3 groups, 10 rats in each group: control group, model group,

and SWP group (SWP). During the experiment, all animals were access to food and water freely, with standard surroundings: 12 h light and shade cycle, 50–55% humidity and temperature at 20–22°C.

In this section, the model of aplastic anemia was established on the basis of previous study.<sup>6</sup> The model group and SWP group were intraperitoneal injected with Cyclophosphamide (CTX) (Baxter International Co., Ltd., Illinois, USA) and 1-Acetyl-2-phenylhydrazine (APH) (Meilun Biotechnology Co., Ltd., Dalian, China), while the control group received an equal volume of phosphate-buffered saline. Additionally, the SWP group was orally administered 22.68g/kg/d SWP, whereas the control and model groups obtained an equal amount of distilled water, lasted for 14 days.

## Peripheral Blood Routine and Histological Analysis

After 14 days, rats were sacrificed under anesthesia and blood sample was collected through the abdominal aorta. The peripheral blood (PB) routine test, including white blood cell count ( $WBC/10^9 \cdot L^{-1}$ ), red blood cell count ( $RBC/10^{12} \cdot L^{-1}$ ), hemoglobin ( $HGB/g \cdot L^{-1}$ ), haematocrit ( $HCT/\%$ ), and platelet count ( $PLT/10^9 \cdot L^{-1}$ ), was applied to evaluate the quantity of blood cells and to diagnosis conditions of blood.<sup>13</sup>

HE staining of femur was also employed to evaluate the medullary hematopoiesis function and the changes of hematopoietic microenvironment.<sup>14</sup> Specific methods are as follows: the fixed femur (decalcified in 5.5g EDTA-2K + 100 mL 4% paraformaldehyde for 20 days in 4°C prior to the following experiments) were embedded in paraffin, and sectioned at 5 mm followed by staining with hematoxylin/eosin. Olympus BH-2 light microscope was used to observe the stained sections of femur tissue (Tokyo, Japan).

## Network Pharmacology Prediction

### Compound Data Preparation and ADME Screening

Traditional Chinese Medicine Systems Pharmacology Database and Analysis Platform (TCMSP) database (<http://lsp.nwu.edu.cn/tcmsp.php>, Ver.2.3), and Bioinformatics Analysis Tool for Molecular mechanism of Traditional Chinese Medicine (BATMAN) (<http://bionet.ncpsb.org/batman-tcm/>, updated January 2016)<sup>15,16</sup> were used to select all candidate compounds of four herbs in SWP. In order to obtain bioactive components contributing to its therapeutic effect, all selected ingredients should meet the principle of ADME: 1. Oral bioavailability (OB)  $\geq 30\%$ , 2. Drug-likeness (DL)  $\geq 0.18$ .<sup>17</sup> In addition, a widely scale data-mining strategy was adopted to replenish some bioactive ingredients, while those with poor pharmacological properties and bad drug ability compounds were removed.<sup>18</sup>

### Targets Fishing and Network Construction

PharmMapper server (<http://lilab-ecust.cn/pharmmapper/>, updated April 10, 2019) was employed to discover the potential targets of SWP bioactive components.<sup>19</sup> We gathered the AA-related targets from following database under the operating condition of “aplastic anemia” and “Homo sapiens”: ①GeneCards (<https://www.genecards.org/>, Ver. 5.0),<sup>20</sup> ②DisGeNET (<https://www.disgenet.org/>, Ver. 6.0),<sup>21</sup> ③OMIM (<http://www.omim.org/>, updated Jun 27, 2017)<sup>22</sup> ④TTD (<http://db.idrblab.org/ttd/>, updated Jan 8, 2020).<sup>23</sup> Herb-Compounds-Target-Pathway network of SWP was displayed by a visualization tool named Cytoscape (ver.3.7.0).<sup>24</sup> The STRING (<https://string-db.org/>, ver. 11.0) database was employed to predict the protein-protein interaction (PPI) in SWP for treating AA, and the operating conditions were “Homo sapiens” and correlation  $\geq 0.7$ .

### GO and KEGG Enrichment Analysis for Targets

To investigate the potential biological pathways and critical targets, our study analyzed the PPI targets with Kyoto Encyclopedia of Genes and Genomes (KEGG), Gene Ontology (GO), and TRRUST (<https://www.grnpedia.org/trrust/>, ver.2).<sup>25</sup> The terms of GO or KEGG with p-value  $\leq 0.05$  were finally screened out for the research.

## Metabolomics Analysis

### Collection and Preparation of Serum Sample

The following methods were employed to prepare serum samples: 100  $\mu$ L aliquot of serum sample were taken from the  $-80^\circ\text{C}$  refrigerator, thawed at  $4^\circ\text{C}$  for 30 minutes. To remove the protein in the sample, 10  $\mu$ L internal standard (0.3 mg/mL 2-chloro-L-phenylalanine) was dispersed in 300  $\mu$ L ice-cold mixture contained methanol and acetonitrile (2/1, v/v).

Then they were vortexed for one minute. Subsequently, the mixtures were handled with concentration under 13,000 rpm and 4 °C for 15 min. 400 µL of the clear supernatant was evaporated, reconstituted with 200 µL of 20% methanol, vortexed for 30s, and sonicated for 2 min. After centrifugation for 10 minutes (13,000 rpm, 4 °C), the supernatant was filtered through a 0.22 µm microfilter and transferred to LC vial. Finally, 10 µL of the supernatant was taken for LC-MS test. Equal volume samples from each group were mixed as Quality Control (QC) in our experiment. Aim to ensure the stability of the samples, the above samples were stored at 4 °C during the LC/MS experiment.

### UPLC-Q-TOF/MS Analysis

An ACQUITY UPLC BEH C18 column (100 mm×2.1 mm, 1.7 µm, Waters, USA) were used for non-targeted metabolites' study to analyze the metabolic profiling under both positive and negative ESI ion modes. Water (containing 0.1% formic acid, v/v) (A) and methanol (B) formed the gradient elution, which procedure was optimized as follows: 0.01 min, 5% B; 1.5 min, 5% B; 3 min, 30% B; 7 min, 60% B; 9min, 90% B; 11 min, 100% B; 12 min, 100% B; 15 min, 5% B. The total procedure time was 15 min, the injection volume was 10 µL, the flow rate was 0.35 mL/min, and the column temperature was 45 °C. The following are the instrument parameters for this experiment: 320°C (+) and 320 °C (–) for ion source temperature; 3500 V (+) and 3100 V (–) for ion spray voltage; 30 PSI for curtain gas; 60–900 (+) and 60–900 (–) for mass scan; 30 eV for collision energy.

### Identification and Quantitative Analysis

In the study, progenesis QI software (Waters Corporation, Milford, USA) was employed to perform standardized preprocessing of metabolomics data.<sup>26</sup> Subsequently, the acceptable ranges of Precursor, fragment and retention time are set as 5 ppm, 10 ppm and 0.02 min, respectively. In order to obtain reliable peak information, we exclude the interference of isotopes, internal standard and noise, and limit the minimum intensity of chromatographic peak to 15% of the base peak intensity. The peaks will be eliminated when their ion intensity equal to 0 exists in more than 60% of samples. The retention time, m/z and MS/MS information are used to automatically match the metabolite information of human metabolite database (HMDB), lipid maps (v2.3) and metlin database to identify the chromatographic peak. Finally, the endogenous metabolites with  $P < 0.05$  were considered as the differential metabolites to distinguish SWP, model and control group after Student's test.

## Target Verification of SWP in Treating AA

### Virtual Docking

To decrease the complexity and improve the accuracy of the constituent-target network, Molecular Operating Environment (MOE 2015.10 software) was further employed in our study to validate the interaction between compounds and critical targets, according to previous studies.<sup>17</sup>

### Elisa

Serum was obtained from the supernatant of blood sample after centrifugation at 4 °C. The levels of serum SPHK-1 (NO. 1229A15), PLD1 (NO. 1228A11), and PLD2 (NO. 1228A09) were monitored by ELISA kits according to the instructions of the manufacturer. All of the ELISA kits were purchased from ZCIBIO Technology Co., Ltd. (Shanghai, China).

### Western Blot Analysis

Bone marrow cells (BMCs) were obtained for Western blot (WB) analysis. BMCs were washed out from rat femurs and tibiae using a 5 mL syringe with PBS (prechilled overnight at 4 °C). The suspension was then centrifuged at 3000 rpm under 4 °C for 15 min. The precipitate was collected, quenched in liquid nitrogen and stored at - 80 °C until analysis. WB analysis was performed as accordance with previous report.<sup>27</sup> In brief, BMCs sample were homogenized on ice in RIPA lysis buffer (Beyotime Biotechnology, China). After the above mixture was centrifuged, the supernatant was collected. Membranes were blotted with primary antibodies, anti-rat p-STAT1 (1:500 dilution), anti-rat GRB2 (1:1000 dilution) or anti-rat GSPT1 (1:1000 dilution), overnight at 4°C. Then incubated with horseradish peroxidase bound secondary antibody for 2 hours. Antibodies p-STAT1 (NO. YP0249), and GSPT1 (NO. YT1619) were obtained from



ImmunoWay Biotechnology Company (USA). Antibodies GRB2 (NO. ba32111) were purchased from Abcam (UK). Immunoreactive proteins were detected by ELX800 and quantified by ClinxChemiScope 6000 System.

## Multivariate Statistical and Pathway Analysis

SPSS 23.0 software was used to analyze the experimental data. An analysis of variance (ANOVA) is performed to obtain statistical significance for comparisons between multiple parameters. The LSD test is performed under the assumption of equal variances; otherwise, Dunnett's T3 test is carried out to data with unequal variances. Statistical significance is established at  $P < 0.05$  or  $P < 0.01$ . We tested the normality of the data. If the data fit the normal distribution, we did homogeneity analysis of variance, otherwise we did Kruskal–Wallis test and Dunn's test. Normally distributed data are displayed by  $\bar{X} \pm SD$  or  $\bar{X} \pm SEM$ , while skewed data are presented as median (min-max). According to our previous study, random forest and SIMCA software package (version 14.0, Umetrics, Umeå, Sweden) was used to observe the metabolic profiles and differential metabolites in different experimental groups under positive and negative mode. As described in previous studies, differential metabolites were sent to Metaboanalyst 4.0 for pathway enrichment analysis and pathway topological analysis.<sup>28</sup>

## Results and Discussion

### Therapeutic Effect of Siwu Paste on AA Induced by CTX + APH

The results of peripheral blood (PB) and Histological examination indicated that we not only successfully established the aplastic anemia model, but also proved that SWP at the dose of this study had a positive effect on AA. Contrasted with control group, the level of WBC, RBC, HCT and PLT in AA model group was reduced obviously ( $P < 0.01$ ). The above indices in SWP increased significantly compared with model group ( $P < 0.05$ ,  $P < 0.01$ ), suggesting that treatment of SWP could relieve the blood deficiency in AA rats. The details are displayed in [Figure 1A](#) and [Figure S1](#).

HE staining clearly shown the structure of periosteum, marrow cavity and cartilage tissue in control group, and abundant cellular components (granulocytes, megakaryocytes, nucleated cells, etc.) were observed in the medullary cavity. However, AA rats had serious medullary cavity injury, including edema of vascular fibrosis and significant fibrosis. After the treatment of SWP, the pathological condition of femur was improved significantly. The myelofibrosis, medullary cavity edema and fat cells were inhibited efficiently in SWP group. It was also observed that the proliferation of nucleated cells increased actively, and the number of erythrocytes in parenchyma vessels increased ([Figure 1B](#)). Overall, all the investigated parameters were changed significantly in AA rats, but they were restored by the SWP treatments.

The pharmacological study displayed the improving anemia and recovering hematopoietic functions effects of SWP treatment on AA animals, that were conformed to previous research.<sup>6,7</sup> It suggests that SWP may be an alternative manner for AA induced by CTX + APH.

## Network Pharmacology Analysis

### Identification of Siwu Paste's Ingredients and Target Genes

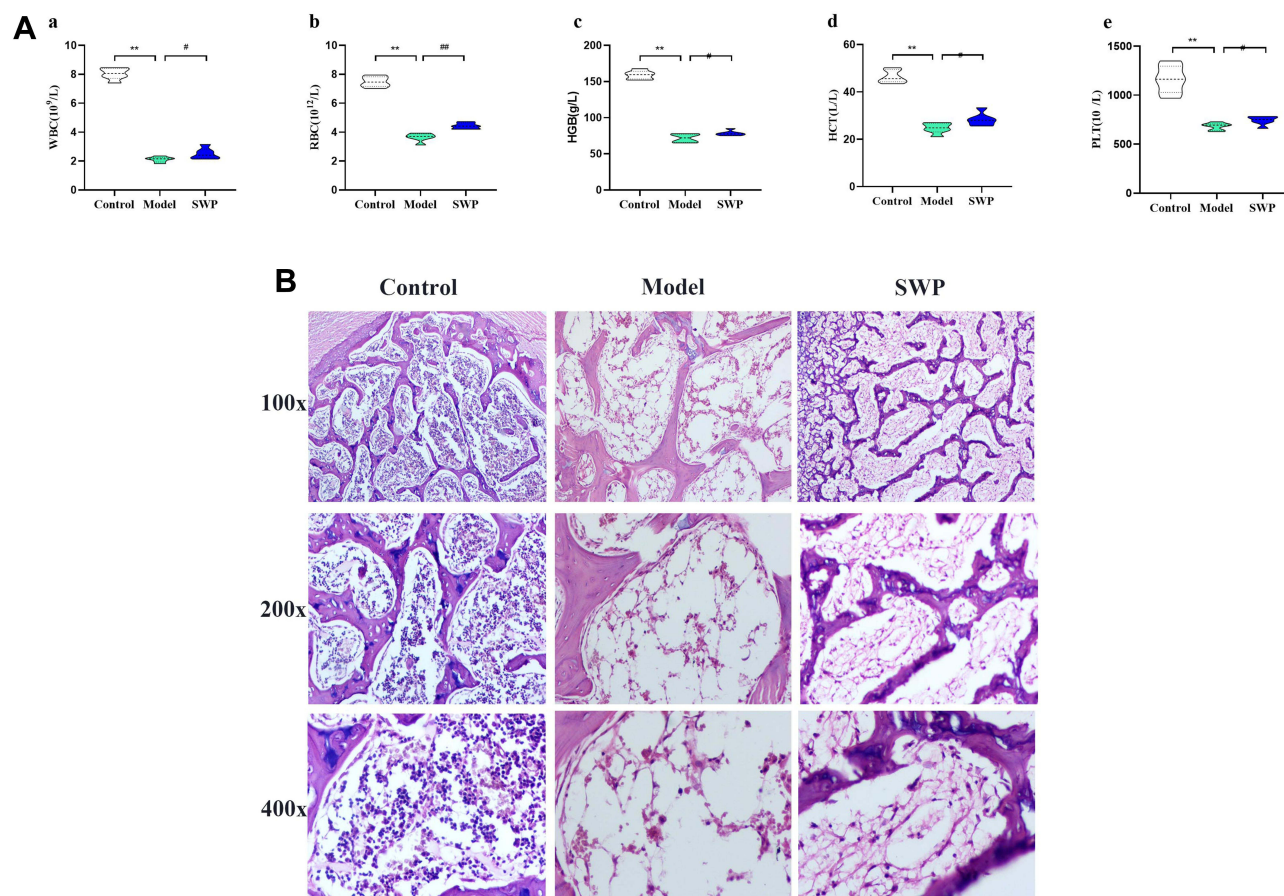
To explore its specific mechanism of anti-anemia, network pharmacology analysis was performed. 230 ingredients were identified in SWP, containing 88 in *Angelicae Sinensis* Radix, 40 in *Rehmanniae radix* preparata, 81 in *Ligusticum chuanxiong* Hort., and 41 in *Cynanchum otophyllum* Schneid., and some repeating compounds were removed ([Table S1](#)). 19 active ingredients were screened from above library by ADEM criteria. According to the literature, eight compounds (Ferulic Acid, vanillin, senkyunolide-C, senkyunolide-D, senkyunolide-E, senkyunolide-A, cis-ligustilide, and senkyunolide-B) were considered to have therapeutic potential for AA, so even if they are below the standard, they are still selected for further study.<sup>8,9</sup> [Table 1](#) provides detailed information on 27 potentially bioactive ingredients. 27 components were imported into the Pharmmapper database in SDF format for target prediction, and their norm fitting values were used for sorting. A total of 317 targets were screened out from the top 100 of each compound. Matching 317 targets with the AA-related targets acquired from GeneCards, DisGeNET, OMIM, and TTD, our study finally identified 64 common targets which considered as the potential gene for SWP in treating AA ([Table 2](#), [Figure 2A](#)).

## Network Construction and Enrichment Analysis

Protein-Protein (PPI) interaction, GO and KEGG analysis were performed in 64 common targets to investigate target function and the potential mechanism of SWP on AA. A view of PPI network is displayed in Figure 2B. In this network, 7 nodes (containing ALB, AKT1, MAPK1, CASP3, HRAS, CAT, IL-2) with the value of degree > 20, were regarded as potential hub target for SWP to ameliorate the hematopoiesis disorder caused by AA.

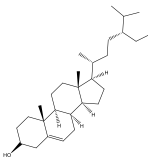
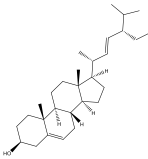
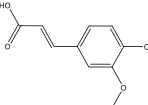
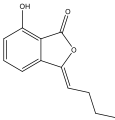
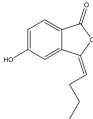
As results shown in GO enrichment (Figure 2C), the top 4 enriched terms are positive regulation of biological process (GO:0048518), cellular protein metabolic process (GO:0044267), regulation of metabolic process (GO:0019222), and regulation of catalytic activity (GO:0050790), all of which belonged to Biological Process. Extracellular vesicle (GO:1903561), vesicle (GO:0031982), and cytosol (GO:0005829) with gene number > 7 belong to terms of GO cellular component. The terms of GO molecular functions mainly included catalytic activity (GO:0003824) and transferase activity, transferring phosphorus-containing groups (GO:0016772). Further TRRUST analysis demonstrates that the 64 targets were primarily regulated by Sp1 transcription factor (SP1, TRR00641), v-rel reticuloendotheliosis viral oncogene homolog A (avian) (RELA, TRR00575), nuclear factor of kappa light polypeptide gene enhancer in B-cells 1 (NF- $\kappa$ B1, TRR00452), and jun proto-oncogene (JUN, TRR00323). Those results indicated that SWP may be mainly involved in regulation of metabolic and protein on treating AA.

In our research, there are 12 KEGG pathway ( $P < 0.05$ ). The top 3 terms are FoxO signaling pathway (map04068), MAPK signaling pathway (map04010), Ras signaling pathway (map04014) which play an important role in the occurrence and development of AA (Figure 2D). A map of the “Herb-Compound-target-pathway” (including 71 nodes and 354 edges) based on KEGG analysis were established to investigate the mechanism of SWP on AA (Figure 2D). In



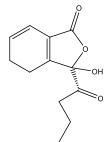
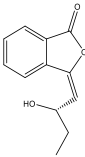
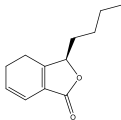
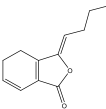
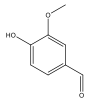
**Figure 1** Therapeutic effect of Siwu Paste on Aplastic Anemia rats. (A) Effects of Siwu paste on peripheral blood routine of Aplastic Anemia Model Rats  $^{*}P < 0.05$ ,  $^{**}P < 0.01$  vs control group;  $^{#}P < 0.05$ ,  $^{###}P < 0.01$  vs model group (n=7–10). WBC: white blood cell count, RBC: red blood cell count, HGB: hemoglobin, HCT: haematocrit, PLT: platelet count. (B) Histological examination of femur (n=3).

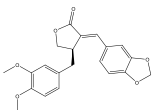
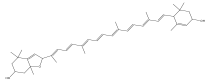
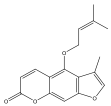
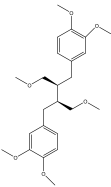
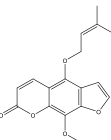
**Table I** A List of the Active Ingredients Among the Four Herbal Medicines in SWP for Network Analysis

NO.	Mol ID	Molecule Name	Formula	MW	Structure	OB (%)	DL	Attribution	Database
1	MOL000358	Beta-sitosterol	C <sub>29</sub> H <sub>50</sub> O	414.79		36.91	0.75	<i>Angelicae Sinensis Radix</i> , <i>Rehmanniae radix preparata</i> , <i>Ligusticum chuanxiong</i> Hort., <i>Cynanchum otophyllum</i> Schneid.	TCMSP, BATMAN-TCM
2	MOL000449	Stigmasterol	C <sub>29</sub> H <sub>48</sub> O	412.77		43.83	0.76	<i>Angelicae Sinensis Radix</i> , <i>Rehmanniae radix preparata</i>	TCMSP, BATMAN-TCM
3	MOL000389	Ferulic Acid	C <sub>10</sub> H <sub>10</sub> O <sub>4</sub>	194.2		54.97	0.06	<i>Angelicae Sinensis Radix</i>	TCMSP
4	MOL002098	Senkyunolide-B	C <sub>12</sub> H <sub>12</sub> O <sub>3</sub>	204.24		62.68	0.08	<i>Angelicae Sinensis Radix</i> <i>Ligusticum chuanxiong</i> Hort.	TCMSP, BATMAN-TCM
5	MOL002143	Senkyunolide-C	C <sub>12</sub> H <sub>12</sub> O <sub>3</sub>	204.24		46.8	0.08	<i>Angelicae Sinensis Radix</i> <i>Ligusticum chuanxiong</i> Hort.	TCMSP, BATMAN-TCM

(Continued)

Table I (Continued).

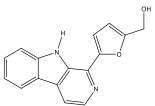
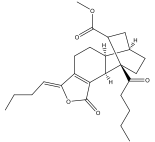
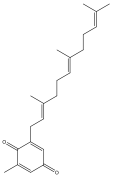
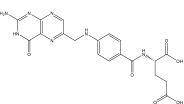
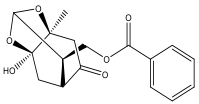
NO.	Mol ID	Molecule Name	Formula	MW	Structure	OB (%)	DL	Attribution	Database
6	MOL002144	Senkyunolide-D	C <sub>12</sub> H <sub>14</sub> O <sub>4</sub>	222.26		79.13	0.1	<i>Angelicae Sinensis Radix</i> <i>Ligusticum chuanxiong</i> Hort.	TCMSP, BATMAN-TCM
7	MOL002145	Senkyunolide-E	C <sub>12</sub> H <sub>12</sub> O <sub>3</sub>	204.24		34.4	0.08	<i>Angelicae Sinensis Radix</i> <i>Ligusticum chuanxiong</i> Hort.	TCMSP, BATMAN-TCM
8	MOL008252	Senkyunolide-A	C <sub>12</sub> H <sub>16</sub> O <sub>2</sub>	192.28		68.28	0.07	<i>Angelicae Sinensis Radix</i> <i>Ligusticum chuanxiong</i> Hort.	TCMSP, BATMAN-TCM
9	MOL002201	Cis-ligustilide	C <sub>12</sub> H <sub>14</sub> O <sub>2</sub>	190.26		51.3	0.07	<i>Angelicae Sinensis Radix</i> <i>Ligusticum chuanxiong</i> Hort.	TCMSP, BATMAN-TCM
10	MOL000635	Vanillin	C <sub>8</sub> H <sub>8</sub> O <sub>3</sub>	152.16		52	0.03	<i>Angelicae Sinensis Radix</i>	TCMSP, BATMAN-TCM

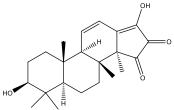
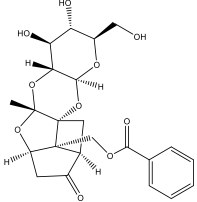
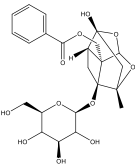
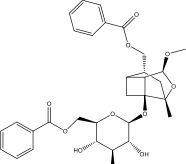
11	MOL005384	Suchilactone	$C_{21}H_{20}O_6$	368.41		57.52	0.56	<i>Angelicae Sinensis Radix</i>	BATMAN-TCM
12	MOL004492	Chrysanthemaxanthin	$C_{40}H_{56}O_3$	584.96		38.72	0.58	<i>Angelicae Sinensis Radix</i>	BATMAN-TCM
13	MOL001942	Isoimperatorin	$C_{16}H_{14}O_4$	270.3		45.46	0.23	<i>Angelicae Sinensis Radix</i>	BATMAN-TCM
14	MOL006812	Phyllanthin	$C_{24}H_{34}O_6$	418.58		33.31	0.42	<i>Angelicae Sinensis Radix</i>	BATMAN-TCM
15	MOL001956	Cnidilin	$C_{17}H_{16}O_5$	300.33		32.69	0.28	<i>Angelicae Sinensis Radix</i>	BATMAN-TCM

(Continued)



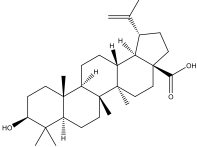
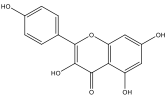
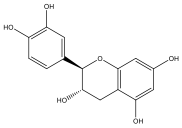
Table I (Continued).

NO.	Mol ID	Molecule Name	Formula	MW	Structure	OB (%)	DL	Attribution	Database
16	MOL002140	Perlolyrine	C <sub>16</sub> H <sub>12</sub> N <sub>2</sub> O <sub>2</sub>	264.3		65.95	0.27	<i>Ligusticum chuanxiong</i> Hort.	TCMSP, BATMAN-TCM
17	MOL002157	Wallichilide	C <sub>25</sub> H <sub>32</sub> O <sub>5</sub>	412.57		42.31	0.82	<i>Ligusticum chuanxiong</i> Hort.	TCMSP
18	MOL002151	Senkyunone	C <sub>22</sub> H <sub>30</sub> O <sub>2</sub>	326.52		47.66	1.15	<i>Ligusticum chuanxiong</i> Hort.	TCMSP
19	MOL000433	Folic acid	C <sub>19</sub> H <sub>19</sub> N <sub>7</sub> O <sub>6</sub>	441.45		68.96	0.71	<i>Ligusticum chuanxiong</i> Hort.	TCMSP
20	MOL001918	Paeoniflorigenone	C <sub>17</sub> H <sub>18</sub> O <sub>6</sub>	318.35		87.59	0.37	<i>Cynanchum otophyllum</i> Schneid.	TCMSP, BATMAN-TCM

21	MOL001919	Palbinone	$C_{22}H_{30}O_4$	358.52		43.56	0.53	<i>Cynanchum otophyllum</i> Schneid.	TCMSP, BATMAN- TCM
22	MOL001921	Lactiflorin	$C_{23}H_{26}O_{10}$	462.49		49.12	0.8	<i>Cynanchum otophyllum</i> Schneid.	TCMSP, BATMAN- TCM
23	MOL001924	Paeoniflorin	$C_{23}H_{28}O_{11}$	480.51		53.87	0.79	<i>Cynanchum otophyllum</i> Schneid.	TCMSP, BATMAN- TCM
24	MOL001930	8-O-benzoylpaeonidanin	$C_{31}H_{36}O_{11}$	584.62		31.27	0.75	<i>Cynanchum otophyllum</i> Schneid.	TCMSP

(Continued)

Table I (Continued).

NO.	Mol ID	Molecule Name	Formula	MW	Structure	OB (%)	DL	Attribution	Database
25	MOL000211	Betulinic acid	C <sub>30</sub> H <sub>48</sub> O <sub>3</sub>	456.78		55.38	0.78	<i>Cynanchum otophyllum</i> Schneid.	TCMSP
26	MOL000422	kaempferol	C <sub>15</sub> H <sub>10</sub> O <sub>6</sub>	286.25		41.88	0.24	<i>Cynanchum otophyllum</i> Schneid.	TCMSP
27	MOL000492	(+)-catechin	C <sub>15</sub> H <sub>14</sub> O <sub>6</sub>	290.29		54.83	0.24	<i>Cynanchum otophyllum</i> Schneid.	TCMSP, BATMAN-TCM

**Table 2** 64 Common Targets from Protein-Protein Interaction Network

NO.	Uniplot	Gene Name	Gene Sympol	NO.	Uniplot	Gene Name	Gene Sympol
1	ACE_HUMAN	Angiotensin-converting enzyme	ACE	33	P00492	Hypoxanthine-guanine phosphoribosyltransferase	HPRT I
2	AKT1_HUMAN	RAC-alpha serine/threonine-protein kinase	AKT1	34	RASH_HUMAN	GTPase HRas	HRAS
3	ALBU_HUMAN	Serum albumin	ALB	35	P11142	Heat shock cognate 71 kDa protein	HSPA8
4	ALDH2_HUMAN	Aldehyde dehydrogenase, mitochondrial	ALDH2	36	IL2_HUMAN	Interleukin-2	IL2
5	ANDR_HUMAN	Androgen receptor	AR	37	IMDH1_HUMAN	Inosine-5-monophosphate dehydrogenase I	IMPDH I
6	Q07960	Rho GTPase-activating protein I	ARHGAP1	38	ITAL_HUMAN	Integrin alpha-L	ITGAL
7	BMP2_HUMAN	Bone morphogenetic protein 2	BMP2	39	Q08881	Tyrosine-protein kinase ITK/TSK	ITK
8	CAH1_HUMAN	Carbonic anhydrase I	CAI	40	KIT_HUMAN	Mast/stem cell growth factor receptor	KIT
9	CASP3_HUMAN	Caspase-3	CASP3	41	NGAL_HUMAN	Neutrophil gelatinase-associated lipocalin	LCN2
10	CASP7_HUMAN	Caspase-7	CASP7	42	TRFL_HUMAN	Lactotransferrin	LTF
11	CATA_HUMAN	Catalase	CAT	43	MK01_HUMAN	Mitogen-activated protein kinase I	MAPK I
12	CD1A_HUMAN	T-cell surface glycoprotein CD1a	CD1A	44	MDM2_HUMAN	E3 ubiquitin-protein ligase Mdm2	MDM2
13	CHK1_HUMAN	Serine/threonine-protein kinase Chk1	CHEK1	45	P08581	Hepatocyte growth factor receptor	MET
14	CATK_HUMAN	Cathepsin K	CTSK	46	NEP_HUMAN	Neprilysin	MME
15	P11511	Cytochrome P450 19A1	CYP19A1	47	MMPI3_HUMAN	Collagenase 3	MMP13
16	DYR_HUMAN	Dihydrofolate reductase	DHFR	48	NOS2_HUMAN	Nitric oxide synthase, inducible	NOS2
17	PYRD_HUMAN	Dihydroorotate dehydrogenase, mitochondrial	DHODH	49	NQO1_HUMAN	NAD(P)H dehydrogenase [quinone] I	NQO1
18	ELNE_HUMAN	Leukocyte elastase	ELANE	50	P09874	Poly [ADP-ribose] polymerase I	PARP1
19	HYES_HUMAN	Epoxide hydrolase 2	EPHX2	51	PDE4D_HUMAN	cAMP-specific 3,5-cyclic phosphodiesterase 4D	PDE4D
20	THRB_HUMAN	Prothrombin	F2	52	HYDROLASE	Urokinase-type plasminogen activator	PLAU
21	FABP4_HUMAN	Fatty acid-binding protein, adipocyte	FABP4	53	ADA17_HUMAN	ADAM 17	PLK1
22	P22830	Ferrochelatase, mitochondrial	FECH	54	PPARG_HUMAN	Peroxisome proliferator-activated receptor gamma	PPARG
23	FGF1_HUMAN	Heparin-binding growth factor I	FGF1	55	PTN11_HUMAN	Tyrosine-protein phosphatase non-receptor type 11	PTPN11
24	FGFR1_HUMAN	Basic fibroblast growth factor receptor I	FGFR1	56	LYAM3_HUMAN	P-selectin	SELP
25	GLCM_HUMAN	Glucosylceramidase	GBA	57	P04179	Superoxide dismutase [Mn], mitochondrial	SOD2
26	P07359	Platelet glycoprotein Ib alpha chain	GPIBA	58	SPRC_HUMAN	SPARC	SPARC
27	G6PI_HUMAN	Glucose-6-phosphate isomerase	GPI	59	STAT1_HUMAN	Signal transducer and activator of transcription I-alpha/beta	STAT1

(Continued)

**Table 2** (Continued).

NO.	Uniprot	Gene Name	Gene Sympol	NO.	Uniprot	Gene Name	Gene Sympol
28	GRB2_HUMAN	Growth factor receptor-bound protein 2	GRB2	60	TGFR2_HUMAN	TGF-beta receptor type-2	TGFR2
29	P00390	Glutathione reductase, mitochondrial	GSR	61	P10828	Thyroid hormone receptor beta	THRB
30	GSTM1_HUMAN	Glutathione S-transferase Mu 1	GSTM1	62	TTHY_HUMAN	Transthyretin	TTR
31	GSTP1_HUMAN	Glutathione S-transferase P	GSTP1	63	VDR_HUMAN	Vitamin D3 receptor	VDR
32	Q9BY41	Histone deacetylase 8	HDAC8	64	P98170	Baculoviral IAP repeat-containing protein 4	XIAP

this network, DG was considered as a principal drug herb for regulating the most multiple compounds, which meet the TCM principles that DG is the sovereign drug in SWP. Moreover, we found that Mitogen-activated protein kinase 1 (MAPK1), RAC-alpha serine/threonine-protein kinase (AKT1), Glutathione S-transferase P (GSTP1), signal transducer and activator of transcription 1-alpha/beta (STAT1), growth factor receptor-bound protein 2 (GRB2) with higher degree also act critical targets for regulating or participating in multiple herbs or signaling pathways. Take GRB2 for example, it involves in multiple pathways related to the blood system, such as FoxO signaling pathway, Phospholipase D signaling pathway (map04072), MAPK signaling pathway, Ras signaling pathway.

GRB2, which links IL3 signaling to the ERK/MAPK proliferative pathway, has been reported to play important functions during the HSPC proliferation, survival and expansion.<sup>29</sup> STAT1 plays an important role in the regulation of erythropoiesis. Studies have shown that STAT1 deficiency leads to increased red blood cell apoptosis.<sup>30</sup> As a stem cell factor (SCF) receptor gene, KIT play a key role in regulating the growth, survival, and differentiation of erythroid progenitors alone, as well as a synergistic effect with erythropoietin (EPO).<sup>31,32</sup> Ratajczak et al, demonstrated that the growth of hematopoietic colony would be inhibited by more than 30%, when the mRNA expression of KIT was blocked in bone marrow mononuclear cells (MNC).<sup>33</sup> Analysis of miRNA differential gene expression in bone marrow revealed that Ras signaling pathways and Rap1 signaling pathway were the most significantly altered pathways between AA patients and healthy controls.<sup>34</sup> The damage of aplastic anemia to bone marrow, HSPC and metabolism is partly due to antigen mediated immune response, which eventually leads to increased oxidative stress or inflammatory response.<sup>35–38</sup> It has been recently reported that FoxO signaling-mediated autophagy and regulation of mitochondrial activity are necessary for maintenance of hematopoiesis homeostasis in HSPC metabolic.<sup>39–41</sup> Our results suggest that promoting erythropoiesis may be an effective strategy for SWP in the treatment of AA.

Those results provide that the herbal combination may have a great range of possible molecular targets than each individual herb, which might help to explain the synergistic of SWP effects in treatment of AA.<sup>17</sup>

## Metabolic Profiles Analysis

### Identification of Differential Metabolites and Multivariate Data Analysis

LC-MS was used to identify endogenous serum metabolic profile between control, model, and SWP group (Figure S2). It can be clearly seen from the random forest method under positive and negative ion modes that the above three groups have been completely separated (Figure 3A). Compared with model group, SWP were closer to control group, as well as the latter one had the trend of regression to the control group. This part indicated that our SWP have the positive regulation on AA. Meanwhile, the QC group was clustered together tightly. It indicated that our metabolic profile is stable and reliable.

In addition, the differences between each two groups were analyzed by orthogonal partial least square-discriminate analysis (OPLS-DA), and the metabolic characteristics of different groups were visualized by SIMCA. In positive (Figure 3B) and negative (Figure 3C) ion modes, there was significant separation between each two groups. If the



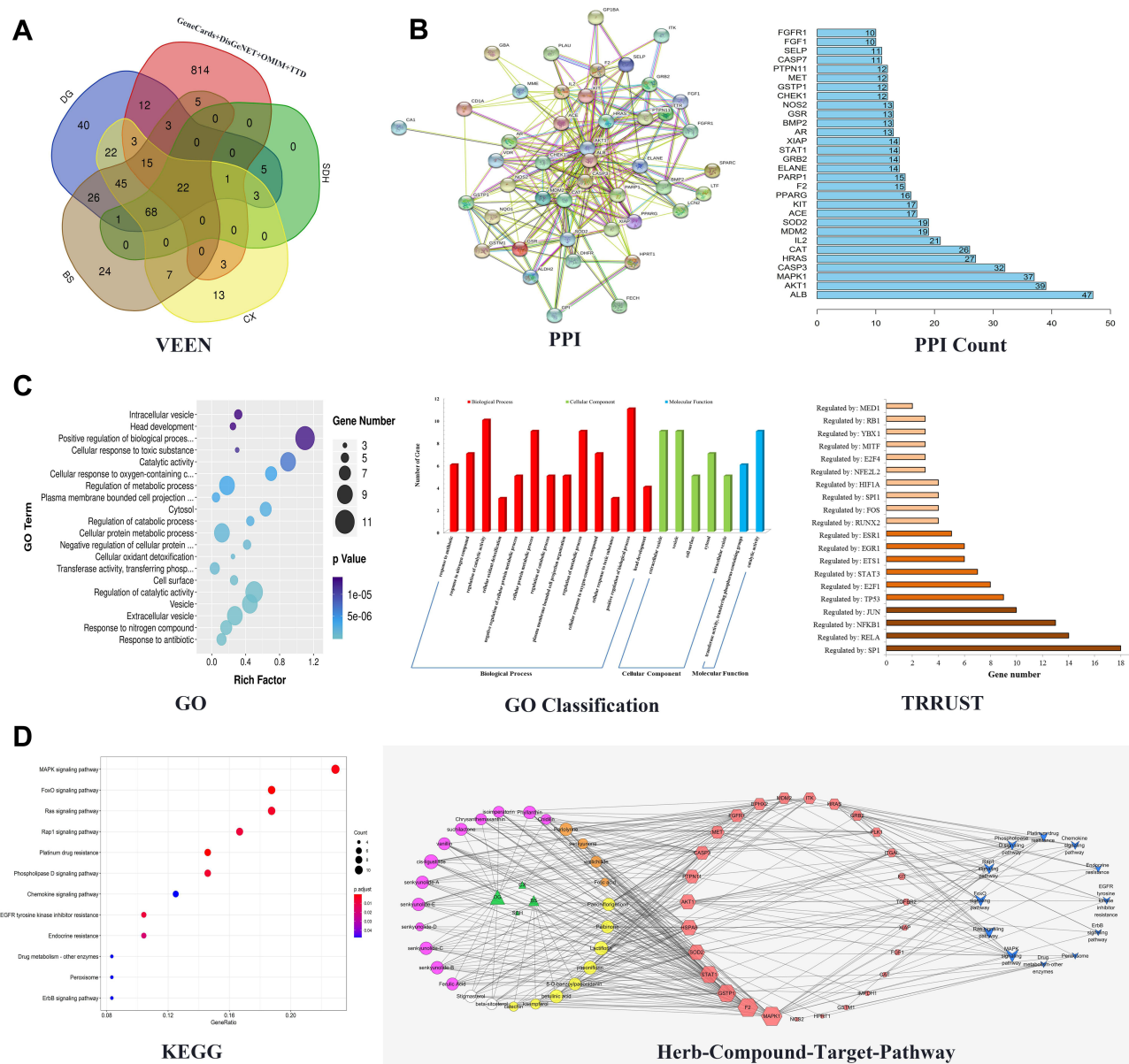


**Figure 2** Network construction and enrichment analysis of Siwu Paste in the treatment of aplastic anemia. **(A)** VENN: Match analysis of 784 potential targets from SWP and 878 AA related targets. **(B)** "Protein-protein interaction network" consist 64 target nodes and 362 degree. "PPI count": The degrees of the first seven nodes (ALB, AKT1, mapk1, CASP3, HRAS, cat and IL-2) were higher than 20. **(C)** GO enrichment analysis of 64 common targets: Size of circle is proportional to the number of gene targets. GO classification: biological process, cellular component and molecular function represented by red, green and blue. **(D)** KEGG enrichment analysis of 64 common targets. "Herb-Compound-Target-Pathway" include 4 herb nodes represented by green triangle, 27 compound nodes, 27 gene target nodes described as a pink hexagon and 12 pathway nodes represented by blue. Yellow, Orange, and purple circles represent compounds from BS, CX and DG, respectively. White circle represents common compounds of DG and SDH.

metabolite meets the conditions of  $VIP > 1$  and  $P < 0.05$ , it will be selected as a potential biomarker. Based on positive ions mode, there are 111 (93 up-/18 down-regulation) and 77 (45 up-/32 down-regulation) biomarkers identified respectively between control and model, and model and SWP. Analogously, 40 (28 up-/12 down-regulation) and 28 (3 up-/25 down-regulation) biomarkers were separately identified under negative ion mode in above mentioned groups (Figure 4, Table S2).

### Metabolic Pathway Analysis

A total of 106 differential metabolites regulated by SWP were further analyzed at Metaboanalyst 4.0 to reveal their functional and metabolic characteristics. 17 metabolic pathways were enriched in our research (Table S3, Figure S3).

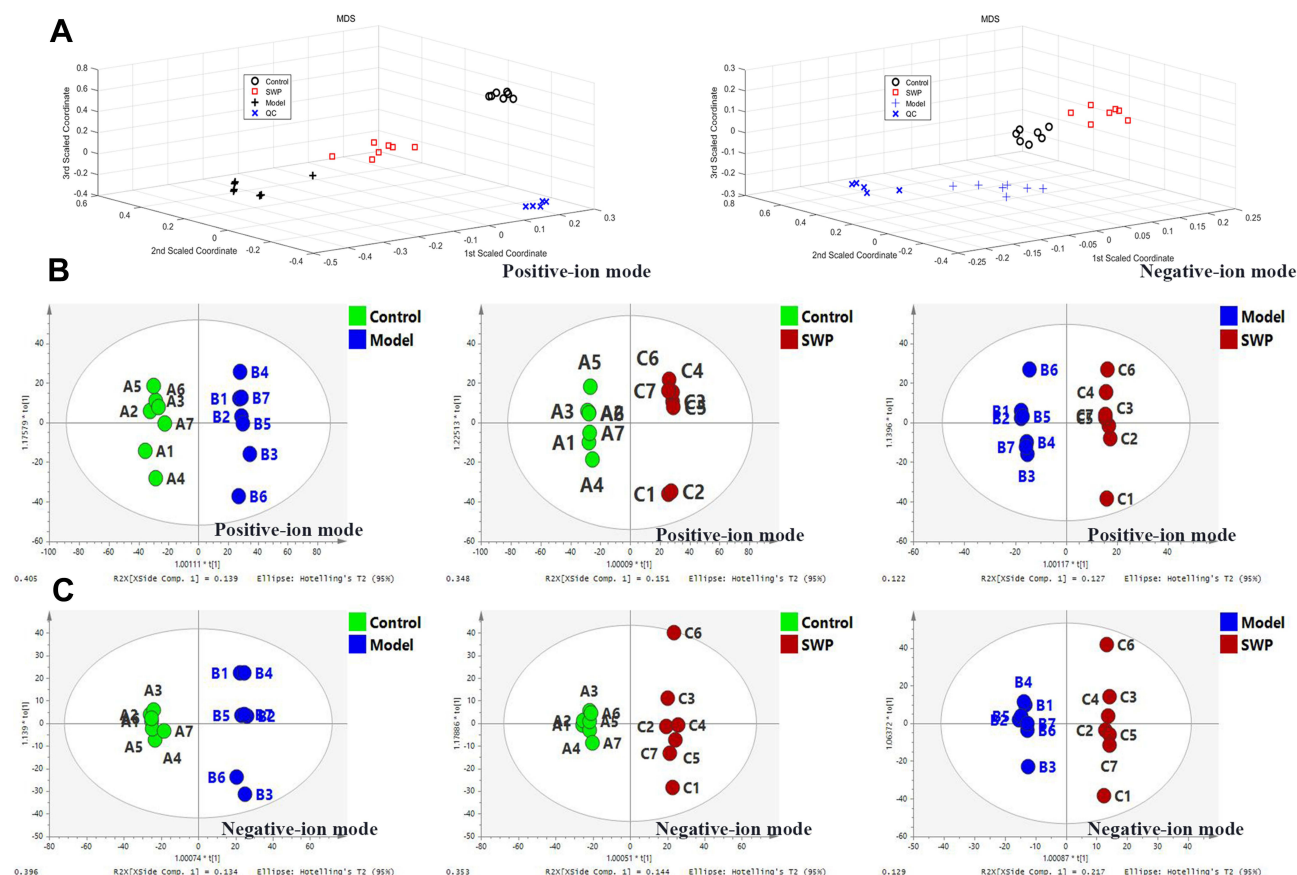


**Figure 3 (A):** Random forest pattern recognition analysis of global serum metabolic profile between the control group, model group, and Siwu Paste group in positive and negative-ion modes. OPLS-DA score plots between the above three groups in positive (B) and negative-ion modes (C), respectively (n=7).

According to the impact value  $> 0.1$ , the top six metabolic pathways, which mainly enriched to lipid metabolism, amino acid, metabolism of terpenoids and polyketides, were obtained (Figure 5). Riboflavin and retinal were involved in Riboflavin metabolism (map00740, impact = 0.5) and Retinol metabolism (map00830, impact = 0.242) respectively. Sphingolipid metabolism (map00600, impact = 0.199) regulated by sphinganine, sphingosine, SM (d18:0/16:1(9Z)), and PE (16:1 (9Z)/P-18:1 (11Z)). Glycerophosphocholine, PC (20:4 (5Z,8Z,11Z,14Z)/P-16:0), PE (16:1 (9Z)/P-18:1 (11Z)), choline, LysoPC (17:0), and LysoPC (24:1 (25Z)) were metabolite nodes in the process of Glycerophospholipid metabolism (map00564, impact = 0.168). PC (20:4 (5Z,8Z,11Z,14Z)/P-16:0) and 15(S)-HPETE were charged in Arachidonic acid metabolism (map00590, impact = 0.1). Niacinamide was participated in the Nicotinate and nicotinamide metabolism (map00760, impact = 0.194). The regulation of SWP on the above 12 metabolites is regarded as a potential biomarker for SWP to reduce AA metabolic disorder (Table 3).

Study testified that Nicotinamide Riboside (NR) and Niacinamide, as nicotinamide adenine dinucleotide (NAD<sup>+</sup>) dietary supplements, recovery hematopoiesis function in mice suffering from hematological failure through reduced mitochondrial activity within HSPC.<sup>42–45</sup> Though products of lipoxygenase in arachidonic acid metabolism are regarded as typical pro-inflammatory, recently study has been proved that 15-HPETE exhibit anti-inflammatory activity by destabilizing TNFmRNA.<sup>46,47</sup> However, abnormal elevation of the membrane-located 15(S)-HPETE can trigger greater levels of oxidative damage to the polyunsaturated fatty acid side-chains, which finally induces the loss of erythrocyte membranes integrity.<sup>48</sup> In this study, the serum level of Nicotinamide Riboside, Niacinamide and 15(s)-HPETE in AA model group was significantly higher than that in control group, whereas the levels of LysoPC (17:0), LysoPC (24:1 (25Z) and PE (16:1 (9Z)/ P-18:1 (11Z)) were decreased markedly ( $P < 0.05$ ). After SWP treatment, the above indexes were significantly restored ( $P < 0.05$ ). Phosphatidylethanolamine (PE) regarded as a potent anti-inflammatory lipid.<sup>49</sup> It has been confirmed that an abundant of lyso-phosphatidylcholine (LPC) such as LysoPC (17:0) and LysoPC (24:1 (25Z)

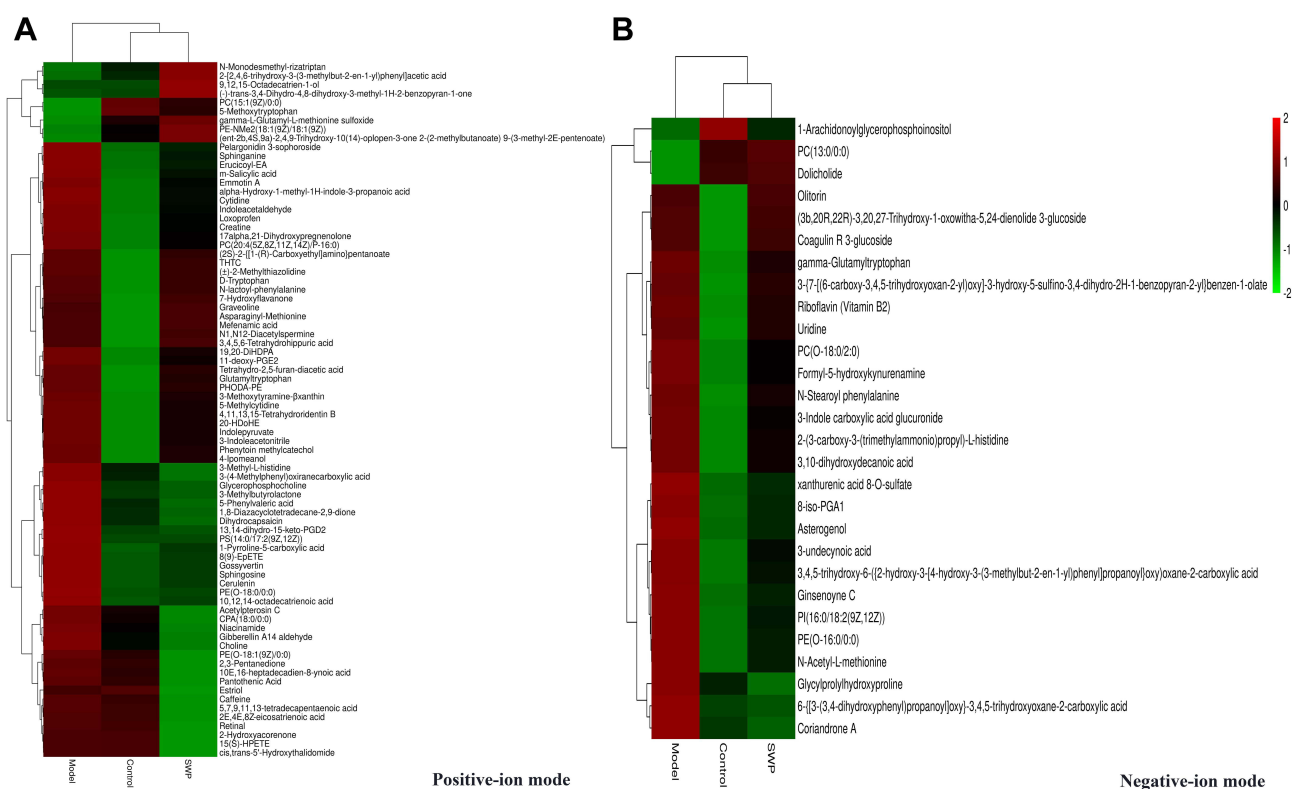


**Figure 4** Comparison of differentially expressed metabolites levels between control group, mode group and Siwu Paste group in positive (A) and negative-ion (B) modes.

in plasma, contributes to driving the activation of inflammatory responses.<sup>50</sup> We speculate that SWP may suppress the inflammation and oxidative damage by restoring the level of PE and LPC and balancing the abnormally increased 15(s)-HPETE under the AA. SWP may also promote the metabolism of Niacinamide for maintenance of adult HSC quiescence. It provides a better hematopoietic microenvironment for promoting hematopoiesis.

Our observations also illustrated that Glycerophospholipid metabolism and Sphingolipid metabolism including PE (16:1 (9Z)/P-18:1 (11Z), Glycerophosphocholine, Sphingosine, Sphinganine, and Sphingosine-1-phosphate, were related to the dysregulation of hematopoietic.<sup>51,52</sup> Orsini's study provides evidence that sphingolipid was participated in TNF $\alpha$ -mediated modulation of TF/miR network and autophagy inhibition in HSPCs, affecting the formation of erythrocytes.<sup>53</sup> Sphinganine is a derivative of Sphingosine. The accumulation of them has been verified to suppresses Bcl-xL expression and downregulates Bcl-2 to enhance apoptosis, which accompanied by the strong inhibition of MAPK cascade.<sup>54–57</sup> Whatmore, Thiet et al, study indicated that a significantly decrease in plasma S1P level in Major-facilitator superfamily transporter 2b (Mfsd2b) knockout mice would result in damaged membrane of erythrocyte and disordered PB.<sup>58</sup> They also found that sphingosine was highly accumulated when the secretion of S1P were block by knockout the Mfsd2b in red blood cell (RBC). On contrary, Sphingosine-1-phosphate (S1P), synthesized by phosphorylation of sphingosine in the presence of sphingosine kinase 1 (SphK1), was shown to have antiapoptotic properties.<sup>54</sup> Our and Wątek's research demonstrate that the levels of Sphingosine and Sphinganine were up-regulated significantly in the model with immune damage mediated by chemotherapeutic drugs, while the concentration of Sphingosine-1-phosphate (S1P) was significantly lower ( $P < 0.05$ ).<sup>59</sup> After the treatment of SWP, the concentration of Sphingosine and Sphinganine was declined significantly compared with model ( $P < 0.05$ ). The Sphingosine-1-phosphate has elevated tendency after treated with SWP with no significance.

## Network Pharmacology and Metabolomics Integration Analysis

To further clarify the molecular mechanism and potential biological pathway of SWP for treatment of AA, we comprehensively analyzed the results of network pharmacology and metabonomics. Firstly, we searched the HMDB





**Table 3** 12 Differentially Metabolites Analysis of Siwu Paste, Model and Control

NO.	Ion-Mode	m/z	Rt (min)	Metabolites	Formula	Mass Error (ppm)	Model vs Control			SWP vs Model		
							Trend	VIP	P	Trend	VIP	P
1	Pos	280.0918	0.82	Glycerophosphocholine	C8H20NO6P	-1.08	↑	1.36	0.0217	↓	1.86	0.0118
2	Pos	104.1073	0.87	Choline	C5H13NO	3.36	↑	1.45	0.0122	↓	2.19	0.0014
3	Pos	123.0554	1.17	Niacinamide	C6H6N2O	0.81	↑	1.22	0.0143	↓	2.15	0.0020
4	Pos	319.2265	8.21	15(S)-HPETE	C20H32O4	-0.8	↑	1.01	0.0140	↓	1.99	0.0059
5	Pos	300.2894	8.28	Sphingosine	C18H37NO2	-1.04	↑	1.12	0.0045	↓	2.05	0.0041
6	Pos	302.305	8.5	Sphinganine	C18H39NO2	-1.04	↑	1.35	0.0001	↓	2.22	0.0012
7	Pos	267.2103	9.34	Retinal	C20H28O	-1.55	↑	1.38	0.0315	↓	2.11	0.0027
8	Pos	606.4484	11.9	LysoPC (24:1(15Z))	C32H64NO7P	-1.43	↓	1.36	0.0001	↑	1.58	0.0411
9	Pos	725.5542	11.64	SM (d18:0/16:1(9Z))	C39H79N2O6P	-3.63	↑	1.31	0.0003	↓	1.54	0.0500
10	Pos	766.5715	11.95	PC (20:4(5Z,8Z,11Z,14Z)/P-16:0)	C44H80NO7P	-3.94	↑	1.02	0.0123	↓	1.8	0.0162
11	Neg	842.5894	9.54	PE (20:1(11Z)/20:2(11Z,14Z))	C45H84NO8P	-2.86	↓	2.38	0.0014	↑	1.22	0.0001
12	Neg	508.3395	10.17	LysoPC (17:0)	C25H52NO7P	-2.74	↓	1.68	0.0014	↑	1.22	0.0232



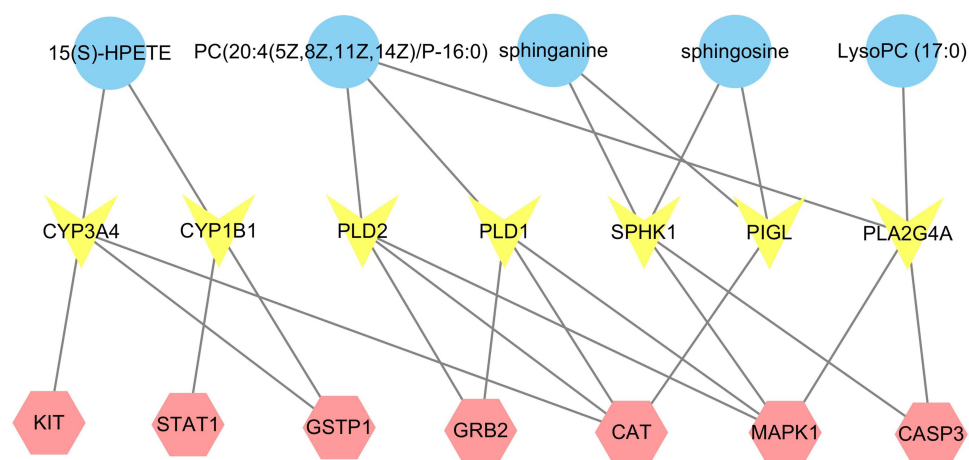


**Figure 6** “Metabolites-enzyme-target network”: Blue circles, pink hexagon, and yellow represent metabolites, target and enzyme, respectively.

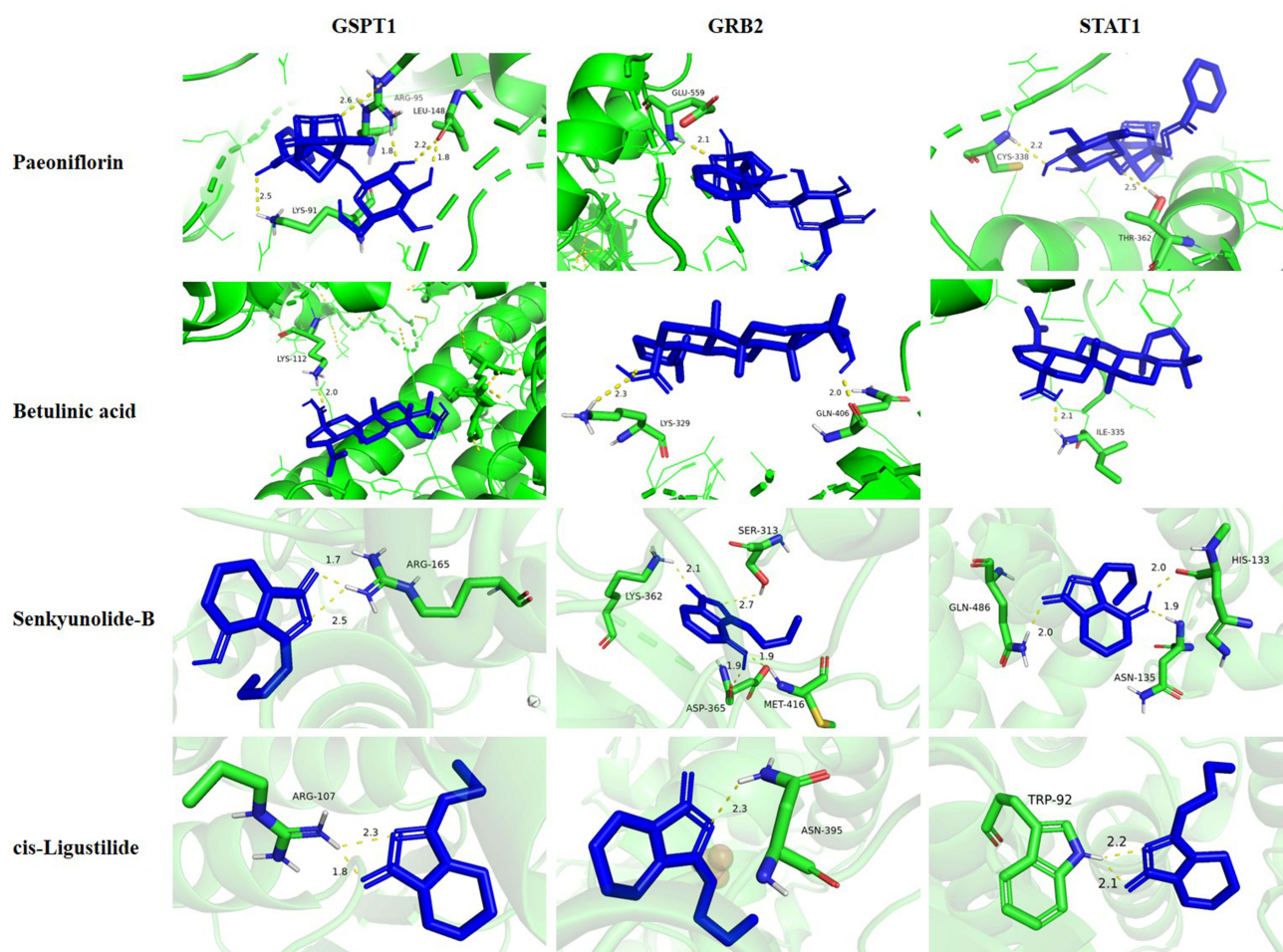


**Figure 7** Virtual docking based on bioactive ingredients of Siwu Paste and therapeutic targets of Aplastic Anemia.

in AA remains unclear, our study suggests that PLD expression is disrupted in chemotherapy-induced AA and that SWP reverses this imbalance. In addition, it is partly consistent with the prediction of our networked pharmacology combined with metabolomics.

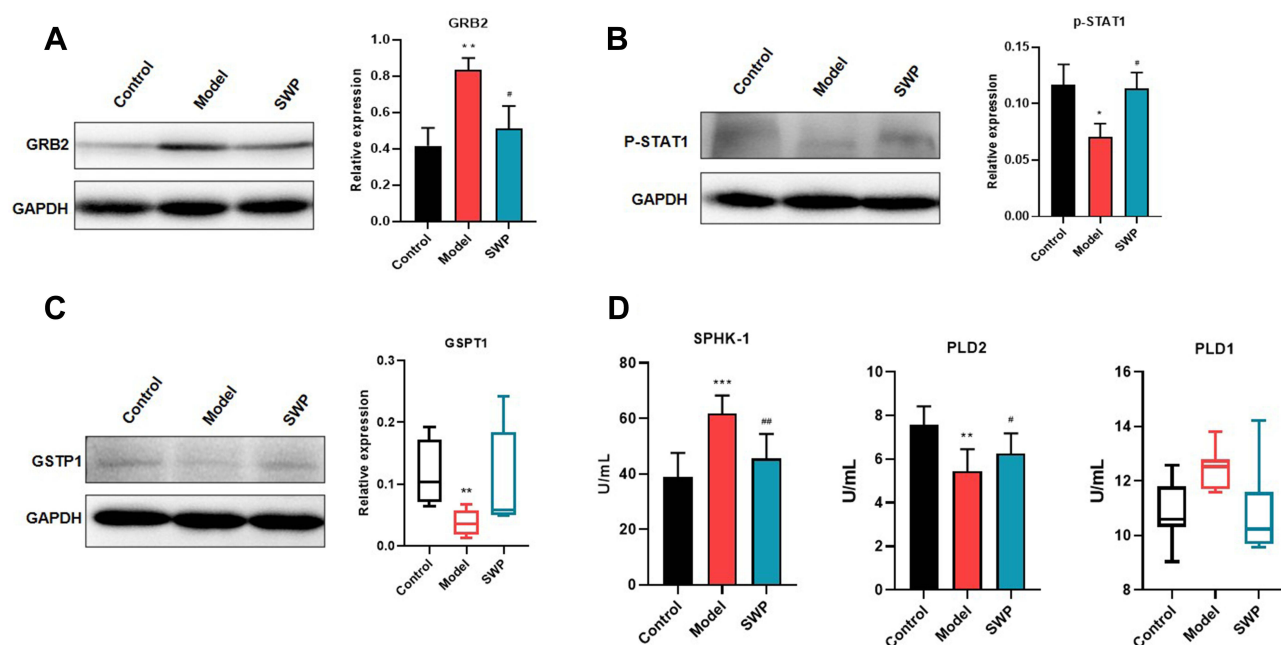


**Figure 8** The experimental validation of Siwu Paste against Aplastic Anemia. The relative protein expression levels of GRB2 (A), p-STAT1 (B) and GSPT1 (C) were monitored by Western Blot. Serum SPHK-1, PLD1 and PLD2 levels were assessed by ELISA (D). The results of GSPT1 and PLD1 were expressed by median (min - max), while other data were expressed by mean  $\pm$  SEM. \* $P < 0.05$ , \*\* $P < 0.01$ , \*\*\* $P < 0.001$  vs control group; # $P < 0.05$ , ## $P < 0.01$  vs model group.

Although we have examined the possible role of SWP in treating AA induced by CTX + APH, there are some limitations in the present study. Due to the limitation of the sample size, we cannot estimate the efficacy of SWP in large samples. Therefore, it is necessary to enlarge the sample size in future experiments. In addition, the potential targets and biological pathways predicted by network pharmacology combined with metabolomics methods need to be validated by more in vitro experiments. Targeting lipid metabolism is also the direction we need to work on in the next step.

## Conclusion

In summary, our research confirmed the positive effect of SWP on aplastic anemia (AA), and enriched the possible pathway of SWP via network pharmacology and metabolomics analysis. In the component-target and PPI network, we identified 27 active compounds from SWP and 64 common proteins associated with AA. Furthermore, MAPK1, CASP3, STAT1, GRB2 and KIT were identified as the hub targets for SWP in treating AA. Metabolomics was employed to characterize the metabolic profiles of APH together with CTX-induced AA rats, attending to identified the endogenous markers that drive molecular mechanisms. SWP improved inflammation and oxidative damage of hematopoietic microenvironment predominantly by significantly down-regulated the elevated levels of 15(s)-HPETE, as well as dramatically up-regulated the levels of LysoPC (17:0), LysoPC (24:1 (25Z)) and PE (16:1 (9Z)/P-18:1 (11Z)). Most importantly, SWP effected hematopoietic by declined the accumulation of Niacinamide, Sphingosine and Sphinganine. The alter of these metabolites mainly involve in Sphingolipid metabolism, Glycerophospholipid metabolism, Arachidonic acid metabolism, Nicotinate and nicotinamide metabolism. Although we have examined the possible role of SWP in treating AA, there are some limitations in the present study. Further vitro and vivo experimental validation will be involved in our next step study.

## Acknowledgments

This work was supported by the Natural Science Foundation of China (No. 81673585, No. 81874493, and No. 81573956); Training Program for Excellent Young Innovators of Changsha (kq1802017); Key Research and Development Project of Changsha Science and Technology (kq1901067); Science Foundation of Hunan Province (2019JJ50345, 2020JJ5325, and 2021168); Program of Survey of Chinese Medicines of China ([2017]66); Research

on the Comprehensive Development and Utilization of Characteristic Traditional Chinese Medicine Resources (2060302); Key Research and Development Project of Hunan Province Science and Technology (2020SK2029, 2020SK2101, 2022ZYC024), and Project of Changsha Technology Innovation Center (kh2004018); and the authors are thankful for the support of Hunan Province traditional Chinese medicine preparation and quality traceability engineering and technology center and 2011 Collaboration and Innovation Center for Digital Chinese Medicine in Hunan.

## Author Contributions

All authors made substantial contributions to conception and design, acquisition of data, or analysis and interpretation of data; took part in drafting the article or revising it critically for important intellectual content (including the work of network pharmacology and metabonomic analysis); agreed to submit to the current journal; gave final approval of the version to be published; and agree to be accountable for all aspects of the work.

## Disclosure

Chun-yu Tang is an employee of Hunan Times Sunshine Pharmaceutical Co., Ltd. The authors declare no other potential conflicts of interest for this work.

## References

1. Cermak J. Aplastic anemia. *Vnitr Lek*. 2018;64(5):501–507. doi:10.36290/vnl.2018.070
2. Ahmed P, Chaudhry QUN, Satti TM, et al. Epidemiology of aplastic anemia: a study of 1324 cases. *Hematology*. 2020;25(1):48–54. doi:10.1080/16078454.2019.1711344
3. Cabannes-Hamy A, Boissel N, Peffault de Latour R, et al. The effect of age in patients with acquired aplastic anaemia treated with immunosuppressive therapy: comparison of adolescents and young adults with children and older adults. *Br J Haematol*. 2018;183(5):766–774. doi:10.1111/bjh.15650
4. Pierri F, Dufour C. Management of aplastic anemia after failure of frontline immunosuppression. *Expert Rev Hematol*. 2019;12(10):809–819. doi:10.1080/17474086.2019.1645003
5. He R, Wang HJ, Ying Z, et al. Siwu decoction improves iron deficiency anemia in infant rats and regulates iron metabolism. *China J Chin Mater Med*. 2017;42(5):944–950. doi:10.19540/j.cnki.cjcmm.20170121.012
6. Du Q, He D, Zeng HL, et al. Siwu Paste protects bone marrow hematopoietic function in rats with blood deficiency syndrome by regulating TLR4/NF- $\kappa$ B/NLRP3 signaling pathway. *J Ethnopharmacol*. 2020;262:113160. doi:10.1016/j.jep.2020.113160
7. He D, Wan D, Shu J, et al. Study progress on compounds, pharmacological action and clinical application of Siwu Decoction. *Pharmacol Clin Chin Mater Med*. 2020;36(6):221–229.
8. Shi XQ, Yue SJ, Tang YP, et al. A network pharmacology approach to investigate the blood enriching mechanism of Danggui buxue Decoction. *J Ethnopharmacol*. 2019;235:227–242. doi:10.1016/j.jep.2019.01.027
9. Wang Y, Guo G, Yang BR, et al. Synergistic effects of Chuanxiong-Chishao herb-pair on promoting angiogenesis at network pharmacological and pharmacodynamic levels. *Chin J Integr Med*. 2017;23(9):654–662. doi:10.1007/s11655-017-2408-x
10. Zhong P, Zhang J, Cui X. Abnormal metabolites related to bone marrow failure in aplastic anemia patients. *Genet Mol Res*. 2015;14(4):13709–13718. doi:10.4238/2015.October.28.33
11. Li PL, Sun HG, Hua YL, et al. Metabolomics study of hematopoietic function of Angelica sinensis on blood deficiency mice model. *J Ethnopharmacol*. 2015;166:261–269. doi:10.1016/j.jep.2015.03.010
12. He Y, Gao T, Li J, et al. Metabonomics study on the effect of Siwu Decoction for blood deficiency syndrome in rats using UPLC-Q/TOF-MS analysis. *Biomed Chromatogr*. 2019;33(11):e4617. doi:10.1002/bmc.4617
13. Válka J, Čermák J. Differential diagnosis of anemia. *Vnitr Lek*. 2018;64(5):468–475. doi:10.36290/vnl.2018.067
14. Marchesi RF, Velloso E, Garanito MP, et al. Clinical impact of dysplastic changes in acquired aplastic anemia: a systematic study of bone marrow biopsies in children and adults. *Ann Diagn Pathol*. 2020;45:151459. doi:10.1016/j.anndiagpath.2019.151459
15. Liu Z, Guo F, Wang Y, et al. BATMAN-TCM: a bioinformatics analysis tool for molecular mechanism of traditional Chinese medicine. *Sci Rep*. 2016;6(1):21146. doi:10.1038/srep21146
16. Ru J, Li P, Wang J, et al. TCMSP: a database of systems pharmacology for drug discovery from herbal medicines. *J Cheminform*. 2014;6(1):13. doi:10.1186/1758-2946-6-13
17. He D, Huang JH, Zhang ZY, et al. A network pharmacology-based strategy for predicting active ingredients and potential targets of Liuwei Dihuang pill in treating type 2 diabetes mellitus. *Drug Des Devel Ther*. 2019;13(1):3989–4005. doi:10.2147/DDDT.S216644
18. Li B, Rui J, Ding X, et al. Exploring the multicomponent synergy mechanism of Banxia Xiexin Decoction on irritable bowel syndrome by a systems pharmacology strategy. *J Ethnopharmacol*. 2019;233:158–168. doi:10.1016/j.jep.2018.12.033
19. Wang X, Shen Y, Shiwei W, et al. PharmMapper 2017 update: a web server for potential drug target identification with a comprehensive target pharmacophore database. *Nucleic Acids Res*. 2017;45(1):356–360. doi:10.1093/nar/gkx374
20. Stelzer G, Rosen N, Plaschkes I, et al. The GeneCards Suite: from gene data mining to disease genome sequence analyses. *Curr Protoc Bioinformatics*. 2016;54(1):1.30.1–1.30.33. doi:10.1002/cpbi.5
21. Piñero J, Ramírez-Anguita JM, Sañch-Pitarch J, et al. The DisGeNET knowledge platform for disease genomics: 2019 update. *Nucleic Acids Res*. 2020;48(D1):D845–d855. doi:10.1093/nar/gkz1021

22. Amberger JS, Hamosh A. Searching Online Mendelian Inheritance in Man (OMIM): a knowledgebase of human genes and genetic phenotypes. *Curr Protoc Bioinform*. 2017;58(1):1.2.1–1.2.12. doi:10.1002/cpbi.27
23. Wang Y, Zhang S, Li F, et al. Therapeutic target database 2020: enriched resource for facilitating research and early development of targeted therapeutics. *Nucleic Acids Res*. 2020;48(D1):D1031–D1041. doi:10.1093/nar/gkz981
24. Merino J, Udler MS, Leong A, et al. A decade of genetic and metabolomic contributions to type 2 diabetes risk prediction. *Curr Diab Rep*. 2017;17(12):135. doi:10.1007/s11892-017-0958-0
25. Han H, Cho JW, Lee S, et al. TRRUST v2: an expanded reference database of human and mouse transcriptional regulatory interactions. *Nucleic Acids Res*. 2018;46(D1):D380–D386. doi:10.1093/nar/gkx1013
26. Jia L, Zuo T, Zhang C, et al. Simultaneous Profiling and holistic comparison of the metabolomes among the flower buds of *Panax ginseng*, *Panax quinquefolius*, and *Panax notoginseng* by UHPLC/IM-QTOF-HDMS(E)-based metabolomics analysis. *Molecules*. 2019;24(11):2188. doi:10.3390/molecules24112188
27. Ying M, Zheng B, Yu Q, et al. *Ganoderma atrum* polysaccharide ameliorates intestinal mucosal dysfunction associated with autophagy in immunosuppressed mice. *Food Chem Toxicol*. 2020;138:111244. doi:10.1016/j.fct.2020.111244
28. Huang JH, He D, Chen L, et al. GC-MS based metabolomics strategy to distinguish three types of acute pancreatitis. *Pancreatology*. 2019;19(5):630–637. doi:10.1016/j.pan.2019.05.456
29. Frelin C, Ofra Y, Ruston J, et al. Grb2 regulates the proliferation of hematopoietic stem and progenitor cells. *Biochim Biophys Acta Mol Cell Res*. 2017;1864(12):2449–2459. doi:10.1016/j.bbamcr.2017.09.018
30. Halupa A, Bailey ML, Huang K, et al. A novel role for STAT1 in regulating murine erythropoiesis: deletion of STAT1 results in overall reduction of erythroid progenitors and alters their distribution. *Blood*. 2005;105(2):552–561. doi:10.1182/blood-2003-09-3237
31. Munugalavadda V, Kapur R. Role of c-Kit and erythropoietin receptor in erythropoiesis. *Crit Rev Oncol Hematol*. 2005;54(1):63–75. doi:10.1016/j.critrevonc.2004.11.005
32. Testa U. Apoptotic mechanisms in the control of erythropoiesis. *Leukemia*. 2004;18(7):1119–1176. doi:10.1038/sj.leu.2403383
33. Ratajczak MZ, Luger SM, Deriel K, et al. Role of the KIT protooncogene in normal and malignant human hematopoiesis. *Proc Natl Acad Sci USA*. 1992;89(5):1710–1714. doi:10.1073/pnas.89.5.1710
34. Adhikari S, Mandal P. Integrated analysis of global gene and microRNA expression profiling associated with aplastic anaemia. *Life Sci*. 2019;228(1):47–52. doi:10.1016/j.lfs.2019.04.045
35. Kordasti S, Costantini B, Seidl T, et al. Deep phenotyping of Tregs identifies an immune signature for idiopathic aplastic anemia and predicts response to treatment. *Blood*. 2016;128(9):1193–1205. doi:10.1182/blood-2016-03-703702
36. Pascutti MF, Erkelens MN, Nolte MA. Impact of Viral Infections on hematopoiesis: from beneficial to detrimental effects on bone marrow output. *Front Immunol*. 2016;7:364. doi:10.3389/fimmu.2016.00364
37. Giudice V, Banaszak LG, Gutierrez-Rodriguez F, et al. Circulating exosomal microRNAs in acquired aplastic anemia and myelodysplastic syndromes. *Haematologica*. 2018;103(7):1150–1159. doi:10.3324/haematol.2017.182824
38. Bissinger R, Bhuyan AAM, Qadri SM, et al. Oxidative stress, eryptosis and anemia: a pivotal mechanistic nexus in systemic diseases. *Febs j*. 2019;286(5):826–854. doi:10.1111/febs.14606
39. Ansó E, Weinberg SE, Diebold LP, et al. The mitochondrial respiratory chain is essential for haematopoietic stem cell function. *Nat Cell Biol*. 2017;19(6):614–625. doi:10.1038/ncb3529
40. Mouchiroud L, Houtkooper RH, Moulán N, et al. The NAD(+)/sirtuin pathway modulates longevity through activation of mitochondrial UPR and FOXO signaling. *Cell*. 2013;154(2):430–441. doi:10.1016/j.cell.2013.06.016
41. Warr MR, Binnewies M, Flach J, et al. FOXO3A directs a protective autophagy program in haematopoietic stem cells. *Nature*. 2013;494(7437):323–327. doi:10.1038/nature11895
42. Vannini N, Campos V, Girotra M, et al. The NAD-booster nicotinamide riboside potently stimulates hematopoiesis through increased mitochondrial clearance. *Cell Stem Cell*. 2019;24(3):405–418.e7. doi:10.1016/j.stem.2019.02.012
43. Moon J, Kim HR, Shin MG. Rejuvenating aged hematopoietic stem cells through improvement of mitochondrial function. *Ann Lab Med*. 2018;38(5):395–401. doi:10.3343/alm.2018.38.5.395
44. Yang Y, Sauve AA. NAD(+) metabolism: bioenergetics, signaling and manipulation for therapy. *Biochim Biophys Acta*. 2016;1864(12):1787–1800. doi:10.1016/j.bbapap.2016.06.014
45. Belenky P, Bogan KL, Brenner C. NAD+ metabolism in health and disease. *Trends Biochem Sci*. 2007;32(1):12–19. doi:10.1016/j.tibs.2006.11.006
46. Rock C, Moos PJ. Selenoprotein P protects cells from lipid hydroperoxides generated by 15-LOX-1. *Prostaglandins Leukot Essent Fatty Acids*. 2010;83(4–6):203–210. doi:10.1016/j.plefa.2010.08.006
47. Ferrante JV, Ferrante A. Novel role of lipoxygenases in the inflammatory response: promotion of TNF mRNA decay by 15-hydroperoxyeicosatetraenoic acid in a monocytic cell line. *J Immunol*. 2005;174(6):3169–3172. doi:10.4049/jimmunol.174.6.3169
48. Calzada C, Rice-Evans C. Ruptured erythrocytes inhibit the oxidation of membranes by 15-hydroperoxy-eicosatetraenoic acid. *FEBS Lett*. 1993;329(1–2):111–115. doi:10.1016/0014-5793(93)80204-8
49. Ireland R, Schwarz B, Nardone G, et al. Unique Francisella phosphatidylethanolamine acts as a potent anti-inflammatory lipid. *J Innate Immun*. 2018;10(4):291–305. doi:10.1159/000489504
50. Taylor LA, Arends J, Hodina AK, et al. Plasma lyso-phosphatidylcholine concentration is decreased in cancer patients with weight loss and activated inflammatory status. *Lipids Health Dis*. 2007;6:17. doi:10.1186/1476-511X-6-17
51. Pernes G, Flynn MC, Lancaster GI, et al. Fat for fuel: lipid metabolism in haematopoiesis. *Clin Transl Immunology*. 2019;8(12):e1098. doi:10.1002/cti2.1098
52. Bansal P, Dahate P, Raghuvanshi S, et al. Current updates on role of lipids in hematopoiesis. *Infect Disord Drug Targets*. 2018;18(3):192–198. doi:10.2174/1871526518666180405155015
53. Orsini M, Chateauvieux S, Rhim J, et al. Sphingolipid-mediated inflammatory signaling leading to autophagy inhibition converts erythropoiesis to myelopoiesis in human hematopoietic stem/progenitor cells. *Cell Death Differ*. 2019;26(9):1796–1812. doi:10.1038/s41418-018-0245-x
54. Young MM, Kester M, Wang HG. Sphingolipids: regulators of crosstalk between apoptosis and autophagy. *J Lipid Res*. 2013;54(1):5–19. doi:10.1194/jlr.R031278



55. Shirahama T, Sakakura C, Sweeney EA, et al. Sphingosine induces apoptosis in androgen-independent human prostatic carcinoma DU-145 cells by suppression of bcl-X(L) gene expression. *FEBS Lett.* **1997**;407(1):97–100. doi:10.1016/S0014-5793(97)00304-9
56. Sakakura C, Sweeney EA, Shirahama T, et al. Suppression of bcl-2 gene expression by sphingosine in the apoptosis of human leukemic HL-60 cells during phorbol ester-induced terminal differentiation. *FEBS Lett.* **1996**;379(2):177–180. doi:10.1016/0014-5793(95)01508-6
57. Jarvis WD, Fornari FA Jr., Auer KL, et al. Coordinate regulation of stress- and mitogen-activated protein kinases in the apoptotic actions of ceramide and sphingosine. *Mol Pharmacol.* **1997**;52(6):935–947. doi:10.1124/mol.52.6.935
58. Vu TM, Ishizu AN, Foo JC, et al. Mfsd2b is essential for the sphingosine-1-phosphate export in erythrocytes and platelets. *Nature.* **2017**;550(7677):524–528. doi:10.1038/nature24053
59. Wątek M, Durnas B, Wollny T, et al. Unexpected profile of sphingolipid contents in blood and bone marrow plasma collected from patients diagnosed with acute myeloid leukemia. *Lipids Health Dis.* **2017**;16(1):235.

## Drug Design, Development and Therapy

Dovepress

### Publish your work in this journal

Drug Design, Development and Therapy is an international, peer-reviewed open-access journal that spans the spectrum of drug design and development through to clinical applications. Clinical outcomes, patient safety, and programs for the development and effective, safe, and sustained use of medicines are a feature of the journal, which has also been accepted for indexing on PubMed Central. The manuscript management system is completely online and includes a very quick and fair peer-review system, which is all easy to use. Visit <http://www.dovepress.com/testimonials.php> to read real quotes from published authors.

Submit your manuscript here: <https://www.dovepress.com/drug-design-development-and-therapy-journal>